Supplementary Material (ESI) for Energy & Environmental Science
This journal is © The Royal Society of Chemistry 2014

Supplementary Information

Solar production of H_2O_2 on reduced graphene oxide-TiO_2 hybrid photocatalysts consisting of earth-abundant elements only

Gun-hee Moon,[a] Wooyul Kim,[a] Alok D. Bokare,[a] Nark-eon Sung,[b] and Wonyong Choi*[a]

[a]Department of Chemical Engineering and School of Environmental Science and Engineering, Pohang University of Science and Technology (POSTECH), Pohang, 790-784, Republic of Korea, E-mail: wchoi@postech.edu.

[b]Pohang Accelerator Laboratory (PAL), Pohang, 790-834, Republic of Korea

Experimental section

Synthetic methods

Graphite oxide was prepared by the complete oxidation of natural graphite (SP-1 grade 200 mesh, Bay Carbon Inc.) using modified Hummers method. A specific amount of graphite oxide was exfoliated into single-layered graphene oxide (GO) in water (200 mL) by sonication (JAC 4020, 400W, Sonic) for 1 hour. 0.4 mL of ammonia solution (Samchun chemicals, 28-30%) and 10 μL of hydrazine hydrate (Aldrich) per mg of GO were added in the GO-dispersed solution to adjust high pH and to reduce GO, respectively. The solution was heated up to 95 ^{o}C with a reflux condenser and kept for 2 hours under slow stirring using a glass encased magnetic stir bar to prohibit the aggregation of reduced graphene oxide (rGO) itself. The solution was cooled down to room temperature and then TiO_2 powder (P25, Degussa) was added. To disperse TiO_2 powder, the solution was sonicated in the ultrasonic bath, and then 4-10 mL of 1 M hydrochloric acid was rapidly injected during fast agitation. The precipitated rGO/TiO_2 composite was washed until neutral pH, dried at room temperature, and treated at 200 ^{o}C under argon gas flow. The photo-deposition of Ag, Au and Pt on TiO_2 was performed in an aqueous solution containing methanol as an electron donor and metal precursors ($AgNO_3$, $HAuCl_4$, and H_2PtCl_6) under UV irradiation for 30 minutes using a 200-W mercury lamp.

Materials characterizations

The UV/Visible absorbance of GO and rGO was measured by a UV/Visible spectrophotometer (Agilent 8453). The change of functional groups on TiO_2, GO, and rGO/TiO_2 was recorded by a Thermo Scientific iS50 FTIR-ATR. Raman spectra of TiO_2, GO, and rGO/TiO_2 were obtained by a BrukerSenterra Raman microscope (BrukerOptics, Inc.) with 532 nm laser excitation. X-ray photoelectron spectroscopy (XPS) analysis with an X-ray source using monochromatic Al (1500 eV) was performed by ESCA LAB250 (VG Scientific). The morphology of rGO/TiO_2 complexed with cobalt phosphate was measured by field emission scanning electron microscopy (FE-SEM, JEOL, JSM), transmission electron microscopy (TEM, JEOL, JEM-2200FS), and electron energy loss spectrum (EELS) analysis with Cs correction. Co K-edge X-ray absorption near edge structure (XANES) were collected on BL8C beamline at the Pohang light source (PLS-II) with a ring current of 200 mA at 3.0 GeV. The monochromatic X-ray beam was obtained from an in-vacuum undulator radiation source through a liquid-nitrogen cooled Si (111) double crystal monochromator. The X-ray absorption spectra for the uniformly dispersed powder samples with a proper thickness were recorded in fluorescence mode using a 7-elements low energy Ge detector (Canberra). To reduce intense fluorescent signal of TiO_2, a 40 mm-width Ar filled plastic bag was placed between the sample and fluorescence detector. Higher order harmonic contaminations were eliminated by detuning the incident X-ray intensity by ~30%. Energy calibration has been simultaneously carried out for each measurement with reference Co metal foil placed in front of the third ion chamber. The data reductions of the experimental spectra XANES were performed through the standard XAFS procedure.

Photocatalyitc activity measurements

20 mg of bare TiO_2, rGO/TiO_2, Au/TiO_2, Ag/TiO_2, and Pt/TiO_2 was dispersed in purified water (38 mL) and 2 mL of 2-propanol (Aldrich) was added as an electron donor. After sonication to completely disperse each samples, the pH of the suspension was adjusted to pH 3.0 by $HClO_4$. Since hydrogen peroxide is very unstable under neutral or high pH, all experiments were carried out at pH 3 condition. The solution was continuously purged by oxygen bubbling while it was stirred in dark for 30 minutes. The reactor was irradiated by a 300-W Xe arc lamp (Oriel) whose light was passed through a 10-cm IR filter and a cutoff filter ($\lambda \geq 320$ nm) under continuous stirring. The incident photon flux was estimated about 1.70 x 10^{-3} einstein/min•L by using ferrioxalate actinometry for UV and visible light ($320 < \lambda < 500$ nm). The solution was continuously purged by oxygen bubbling during the irradiation. 1.0 M of potassium phosphate buffer solution was prepared by mixing potassium phosphate monobasic (Aldrich, 99.99 %) and phosphoric acid (Aldrich, ≥ 85 wt% in H_2O, ≥ 99.999% trace metal basis). 20 mg of bare TiO_2, rGO/TiO_2, Au/TiO_2, Ag/TiO_2, and Pt/TiO_2 was dispersed in 0.1 M of buffer solution (4 mL of potassium phosphate buffer solution + 34 mL of purified water) and 2 mL of 2-propanol was added. The pH of the solution was finally adjusted to pH 3.0 by $HClO_4$. All experimental procedures were the same to those without adding phosphate anions. For the decomposition tests of H_2O_2, 20 mg of each samples was dispersed in 40 mL of H_2O_2 solution (5 mM) in the presence/absence of phosphate anions and was irradiated for 90 minutes under O_2-equlibrated conditions. In dark, the decomposition tests with 5 mg of Pt/TiO_2 (1 wt%) and 10 mg of MnO_2 were done in 40 mL of H_2O_2 solution (5 mM) in the presence/absence of phosphate anions for 40 minutes, respectively. In-situ formation of cobalt phosphate (CoPi) was followed by the addition of 0.124 mL of cobalt solution (0.2 g of cobalt perchlorate hexahydrate (Aldrich) in 20 mL of purified water) into 0.1 M of potassium phosphate buffer solution containing 20 mg of samples without adding 2-propanol under continuous O_2 (g) or Ar (g) purging conditions.

The concentration of hydrogen peroxide was estimated using DPD method. 1 mL of sample aliquots was collected by a syringe during the irradiation and filtered by 0.45 μm PTFE filter (Millipore). Depending on the concentration of H_2O_2 produced, the different amount of samples was added to avoid exceeding the detection limit of DPD method. The stock solutions of N,N-diethyl-1,4-phenylene-diamine sulfate (DPD, 97%, Aldrich), peroxidase (POD, horseradish, Aldrich), and sodium phosphate buffer were prepared as follows. 0.1 g of DPD was dissolved in 10 mL of 0.1 N H_2SO_4 solution and 5 mg of POD was dissolved in 5 mL of purified water. The POD solution was kept in a fringe and was prepared once every five days. Sodium phosphate buffer solution was made by mixing of 99.7 mL of purified water, 87.7 mL of 1 M monobasic sodium phosphate (Aldrich) solution, and 12.6 mL of 1 M dibasic sodium phosphate heptahydrate (Aldrich) solution. Based on 1 mL of sample aliquots, 0.4 mL of phosphate buffer, 1.12 mL of water, 1 mL of sample aliquots, 0.05 mL of DPD, and 0.05 mL of POD were mixed and kept under vigorous stirring for 90 seconds. Depending on the concentration of H_2O_2, the ratio of sample aliquot/water was changed. The calibration curves of the concentration of H_2O_2 were also obtained relying on the different range of H_2O_2 concentration. The absorbance was measured at 551 nm by UV/visible spectrophotometer.

(Photo) Electrochemical tests

The slurry-type photocurrent was measured by a three-electrode system connected to a potentiostat (Gamry, Reference 600). Pt wire, graphite rod, and Ag/AgCl were utilized as a working electrode, a counter electrode, and a reference electrode, respectively. The photocatalyst suspension (1.0 g/L, 0.1 M $NaClO_4$, pH 1.8) was irradiated by a 300-W Xe arc lamp with a UV cutoff filter ($\lambda \geq 320$ nm) in the presence of Fe^{3+} as an electron shuttle. The photocurrent was collected with a Pt electrode biased at +0.7 V (vs Ag/AgCl).

The working electrode was fabricated by immobilizing samples on the FTO glass by the doctor blade method (Ethanol was utilized.) followed by heating at 200 ^{o}C under argon gas flow. The catalyst mass loaded on the FTO glass was measured after detaching the coated catalyst by a razor blade: 0.3 mg was measured for each electrode. Pt wire and Ag/AgCl were utilized as a working electrode and a reference electrode, respectively. Photocurrent responses with light on and off were measured by a three-electrode system connected to a potentiostat (Gamry, Reference 600). All photoelectrochemical measurements were performed as follows: $pH_i = 3.0$, $[KClO_4] = 0.1$ M, $\lambda > 320$ nm, Pt as a counter electrode, at the applied bias of + 0.86 V (vs. Ag/AgCl), and under continuous argon gas purging. Linear sweep voltammetry of TiO_2, TiO_2/CoPi, rGO/TiO_2, and rGO/TiO_2/CoPi was obtained in 0.1 M of potassium phosphate buffer solution (pH 7.0) at a scan rate of 20 mV/s under Ar-saturated condition in dark. The photodeposition of CoPi was followed before the measurement.

Table S1 Elementary reaction steps involved in the photocatalytic generation of H_2O_2.

Eq.	Reaction		Ref.
1	$TiO_2 + hv \rightarrow e_{cb}^- + h_{vb}^+$		1
2	$O_2 + e_{cb}^- \rightarrow O_2^{-\bullet}$	$E^0 = - 0.33$ V	1
3	$O_2 + H^+ + e_{cb}^- \rightarrow HO_2\bullet$	$E^0 = -0.046$ V	2
4	$HO_2\bullet + H^+ + e_{cb}^- \rightarrow H_2O_2$	$E^0 = 1.44$ V	2
5	$2HO_2\bullet \rightarrow H_2O_2 + O_2$		3
6	$O_2 + 2H^+ + 2e_{cb}^- \rightarrow H_2O_2$	$E^0 = 0.695$ V	2
7	$HO\bullet + H^+ + e_{cb}^- \rightarrow H_2O$	$E^0 = 2.81$ V	2
8	$2HO\bullet \rightarrow H_2O_2$		4
9	$H_2O_2 + e_{cb}^- + H^+ \rightarrow H_2O + \bullet OH$	$E^0 = 0.71$ or 1.14 V	2
10	$H_2O_2 + 2H^+ + 2e_{cb}^- \rightarrow 2H_2O$	$E^0 = 1.763$ V	2
11	$H_2O_2 + h_{vb}^+ \rightarrow H^+ + HO_2\bullet$		5
12	$H_2O_2 + 2h_{vb}^+ \rightarrow O_2 + 2H^+$		4
13	$H_2O_2 + HO_2^- \rightarrow H_2O + O_2 + OH^-$		6
14	$2Pt + H_2O_2 \rightarrow 2Pt(OH)$		7
15	$2Pt(OH) + H_2O_2 \rightarrow 2Pt(H_2O) + O_2$		7
16	$2H^+ + 2e_{cb}^- \rightarrow H_2$	$E^0 = 0$ V	6
17	$O_2 + 4e_{cb}^- + 4H^+ \rightarrow 2H_2O$	$E^0 = 1.23$ V	6

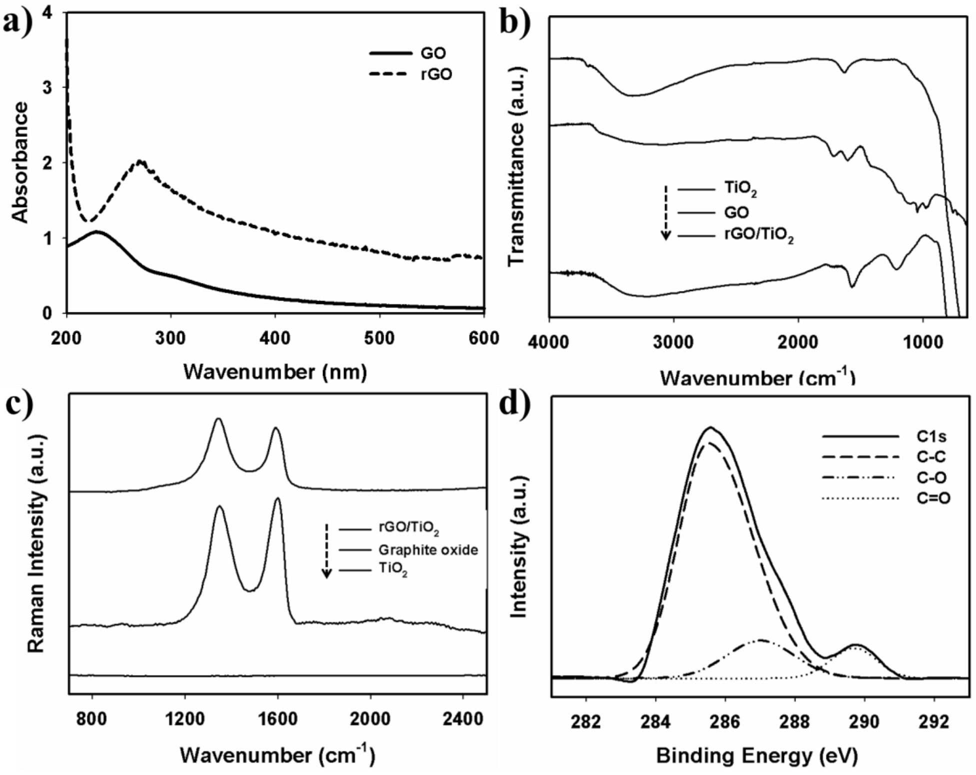

Fig. S1 (a) UV/Visible absorption spectra of the GO and rGO solution. (b) FT-IR and (c) Raman spectra of TiO_2, GO, and rGO/TiO_2 (10 wt%). (d) The deconvoluted XPS spectrum of C1s band for the rGO/TiO_2 (10 wt%).

Two peaks of GO at 230 and 305 nm are ascribed to the π-π* transition of sp^2 carbon networks and the n-π* transition of carbonyl groups, respectively in the UV/Visible absorption spectra (Fig. S1a). After reduction, the peak near 230 nm is shifted to 270 nm due to the recovery of C=C bonds, and the peak near 305 nm almost disappears.[8] The functional groups of TiO_2, GO, and rGO/TiO2 are monitored in the FT-IR spectra (Fig. S1b). The characteristic bands of oxygen-containing functional groups observed in GO (800–2000 cm^{-1}) are effectively removed after reduction.[8] The degree of graphitization (G band) and disorder (D band) of carbon element in TiO_2, GO, and rGO/TiO2 is also measured by Raman spectroscopy (Fig. S1c).[9] The G and D band are not observed in bare TiO_2, but the intensity ratio of D to G band increase after reduction, which indicates that the defect sites are introduced by the decrease of the sp^2 domain size due to its splitting into fragments or the interaction with TiO_2 nanoparticles. The XPS shows the binding energy of C1s corresponding to C-C, C-O, and C=O which are assigned to 285.5, 287.0, and 289.7 eV, respectively, in the rGO/TiO2 composite (Fig. S1d).[10] Despite the complete reduction of GO, oxygen containing functional groups are still observable.

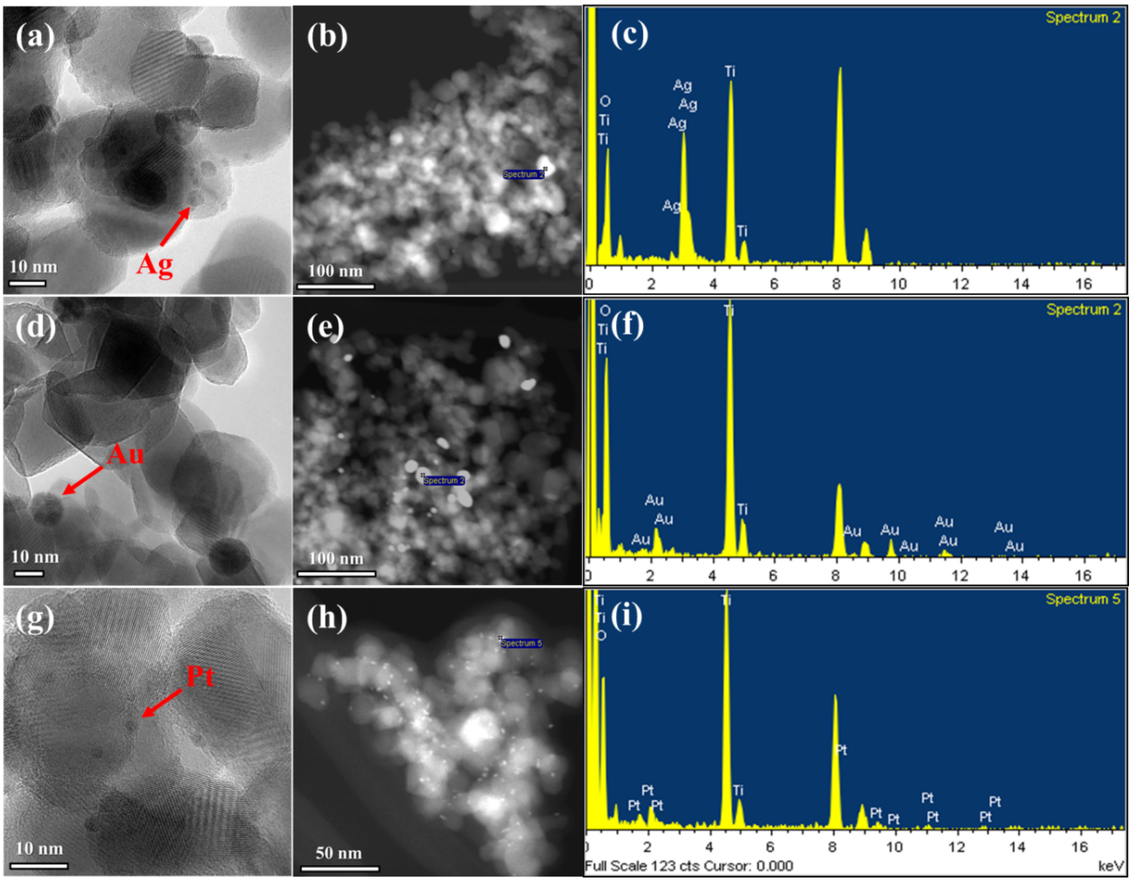

Fig. S2 (a, d, g) HR-TEM images and (b, e, h) HADDF images of Ag/TiO_2, Au/TiO_2, and Pt/TiO_2, respectively. (c, f, i) Spot-profile EDX spectra of a silver nanoparticle, a gold nanoparticle, and a platinum nanoparticle on TiO_2, respectively. Each spot is marked on HADDF images.

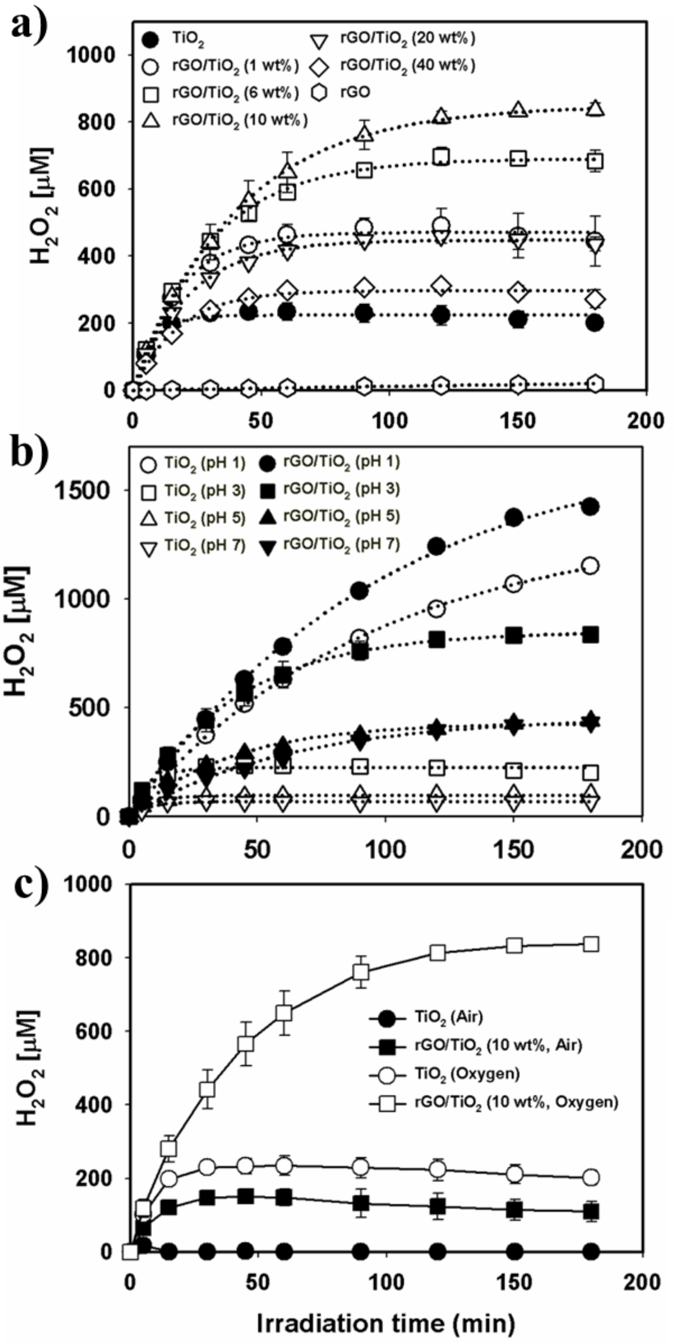

Fig. S3 (a) The photocatalytic formation of H_2O_2 depending on the rGO content loaded on TiO_2 under O_2-equilibrated condition. (b) The photocatalytic generation of H_2O_2 at different pH values under O_2-equilibrated condition. (c) Comparison of the photocatalytic formation of H_2O_2 under air- and O_2-equilibrated conditions with TiO_2 and rGO/TiO_2. The experimental conditions were as follows: 0.5 g/L of catalyst, 5 vol% of 2-propanol, $pH_i = 3.0$ (except for (b)), and $\lambda \geq 320$ nm.

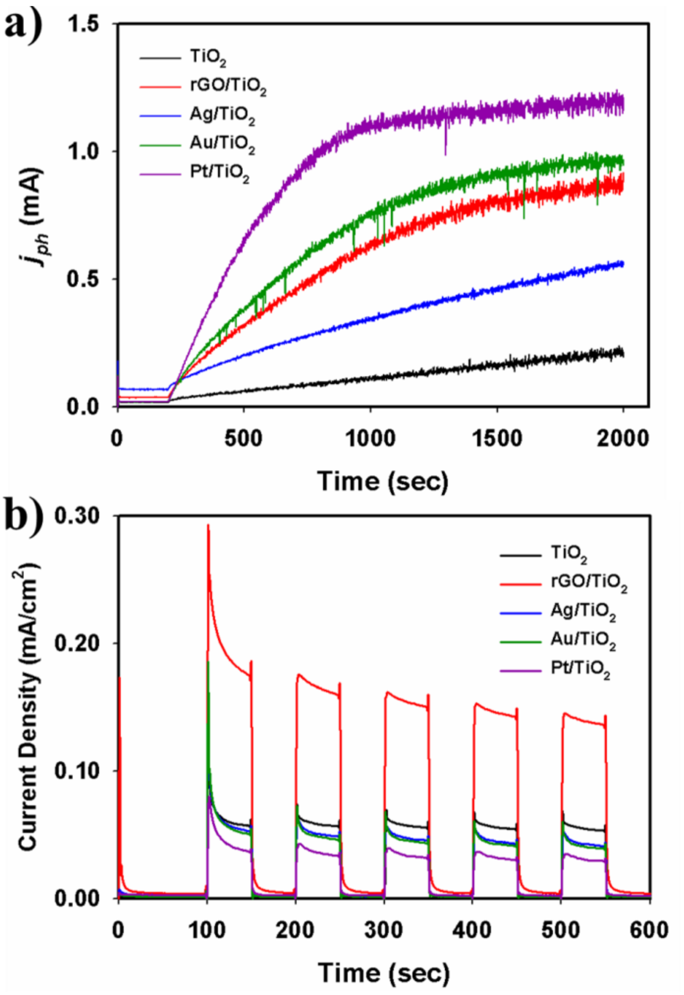

Fig. S4 (a) Time-dependent Fe^{3+}-mediated photocurrent collected on a Pt electrode for TiO_2, rGO/TiO_2 (10 wt%), Ag/TiO_2 (1 wt%), Au/TiO_2 (1 wt%), and Pt/TiO_2 (1 wt%). The dark current was negligible in all cases. The experimental conditions were as follows: 1.0 g/L catalyst, $[Fe^{3+}] = 1$ mM, $pH_i = 1.8$ by $HClO_4$, $\lambda \geq 320$ nm, $[NaClO_4] = 0.1$ M, Pt electrode held at + 0.7 V vs Ag/AgCl, and under a continuously Ar-purged system. (b) Photocurrent responses with light on-and-off for TiO_2, rGO/TiO_2 (6 wt%), Ag/TiO_2 (1 wt%), Au/TiO_2 (1 wt%), and Pt/TiO_2 (1 wt%) electrodes. All photoelectrochemical measurement conditions were as follows: $pH_i = 3.0$, $[KClO_4] = 0.1$ M, $\lambda > 320$ nm, Pt as a counter electrode, at the applied bias of + 0.86 V (vs. Ag/AgCl), and under continuous Ar purging.

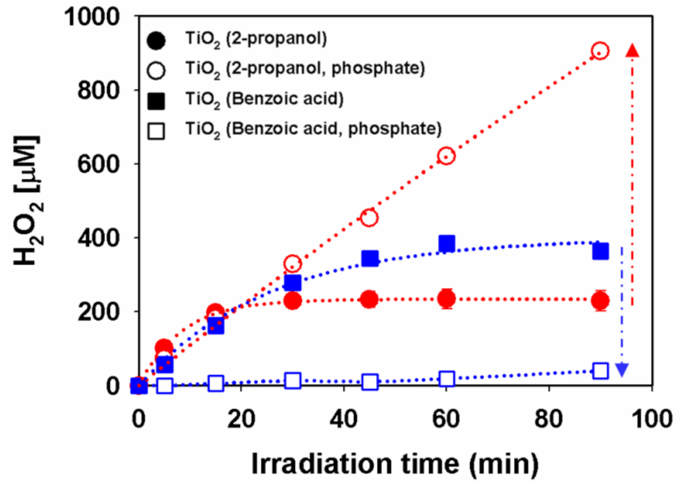

Fig. S5 The photocatalytic production of H_2O_2 depending on the presence of phosphate and the kind of electron donors. The experimental conditions were as follows: $[TiO_2]$ = 0.5 g/L, 5 vol% of 2-propanol or 0.5 mM of benzoic acid, $pH_i = 3.0$, [phosphate] = 0.1 M, O_2-equilibrated, and $\lambda \geq 320$ nm.

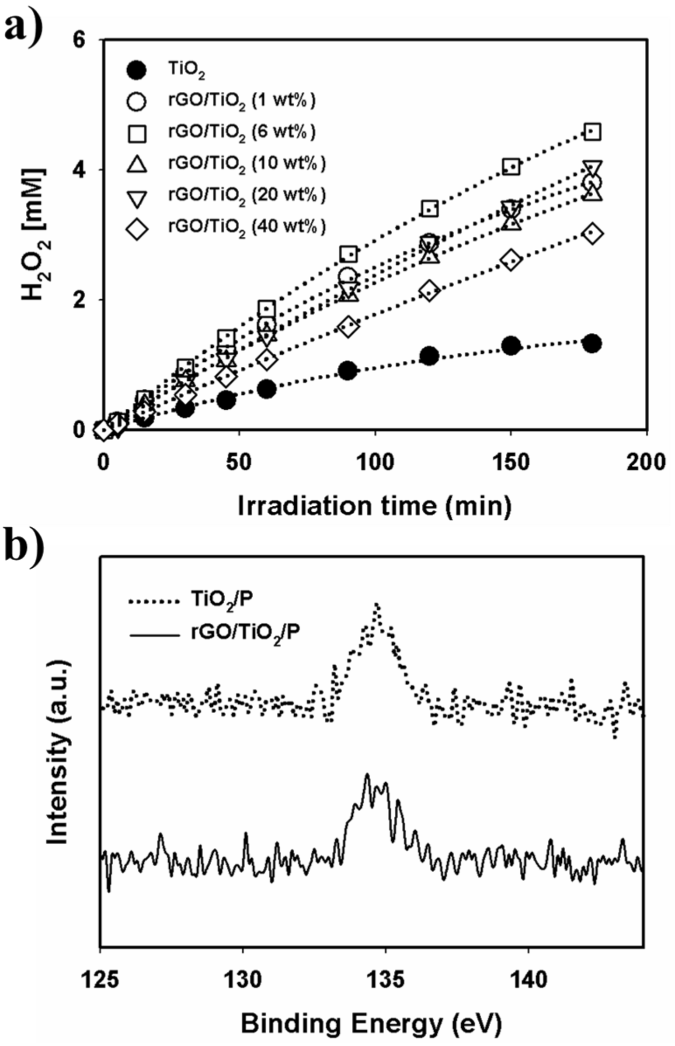

Fig. S6 (a) The photocatalytic formation of H_2O_2 depending on rGO contents in the presence of phosphate. The experimental conditions were as follows: 0.5 g/L of catalyst, 5 vol% of 2-propanol, $pH_i = 3.0$, [phosphate] = 0.1 M, O_2-equilibrated, and $\lambda \geq 320$ nm. (b) XPS spectra of P2p band originated from phosphate complexed on TiO_2 and rGO/TiO_2 (6 wt%).

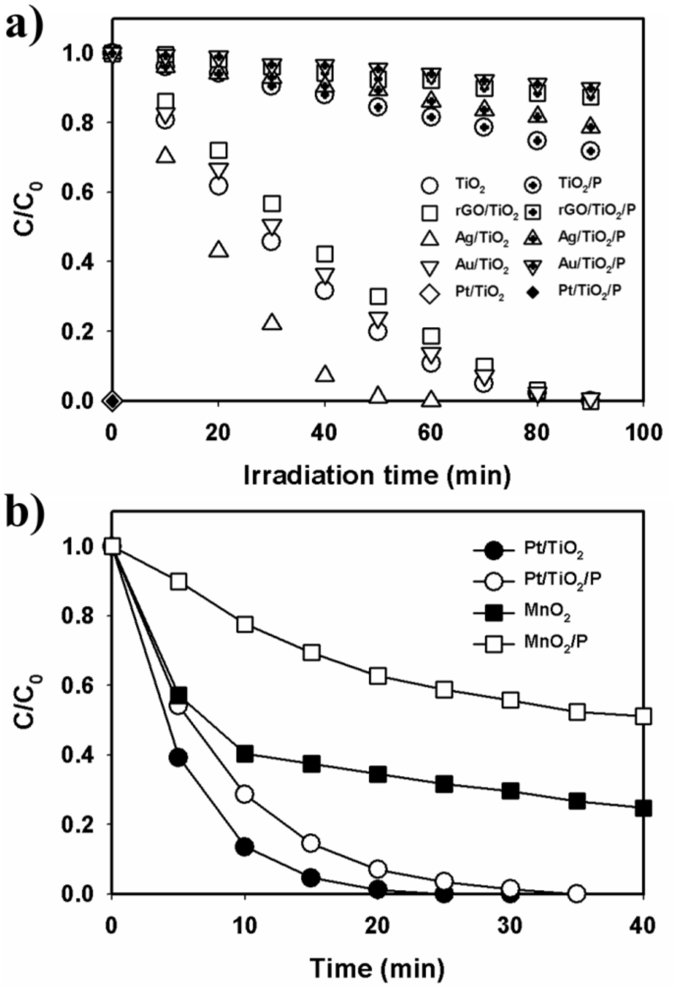

Fig. S7 (a) The photocatalytic decomposition of H_2O_2 in the presence/absence of phosphate for TiO_2, rGO/TiO_2 (6 wt%), Ag/TiO_2 (1 wt%), Au/TiO_2 (1 wt%), and Pt/TiO_2 (1 wt%) during the irradiation. The experimental conditions were as follows: 0.5 g/L of catalyst, $[KP_i] = 0.1$ M, $[H_2O_2]_0 = 5$ mM, $pH_i = 3.0$, and O_2-saturated condition. (b) The catalytic decomposition of H_2O_2 on the Pt/TiO_2 and MnO_2 in the presence/absence of phosphate in dark. The experimental conditions were as follows: 5 mg of Pt/TiO_2 (1 wt%) and 10 mg of MnO_2, $[KP_i] = 0.1$ M, $[H_2O_2]_0 = 5$ mM, $pH_i = 3.0$, and air-saturated condition.

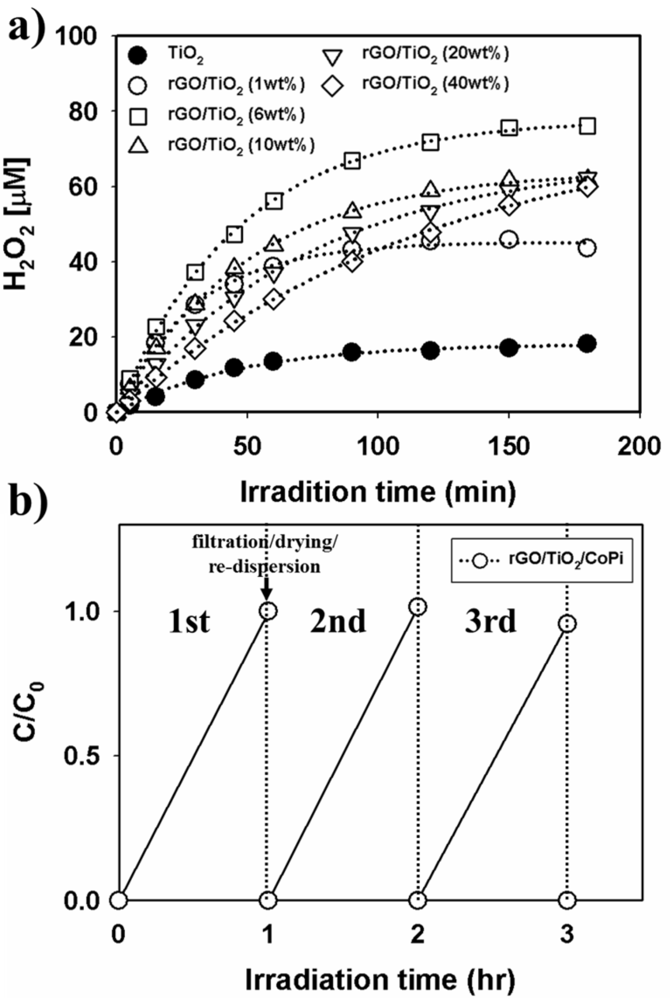

Fig. S8 (a) The photocatalytic formation of H_2O_2 depending on the rGO content in the presence of phosphate and cobalt ions. (b) Repeated runs of H_2O_2 generation in the UV-irradiated suspension of rGO/TiO_2/CoPi. The experimental conditions were as follows: 0.5 g/L of catalyst, 0.124 mL of cobalt perchlorate solution (1 g/100 mL), $pH_i = 3.0$, [phosphate] = 0.1 M, O_2-equilibrated, and $\lambda \geq 320$ nm.

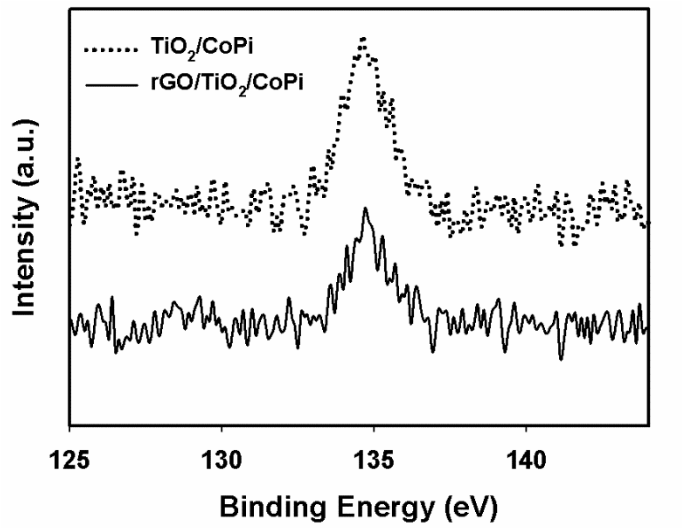

Fig. S9 The XPS spectra of P2p band for TiO_2/CoPi and rGO/TiO_2/CoPi.

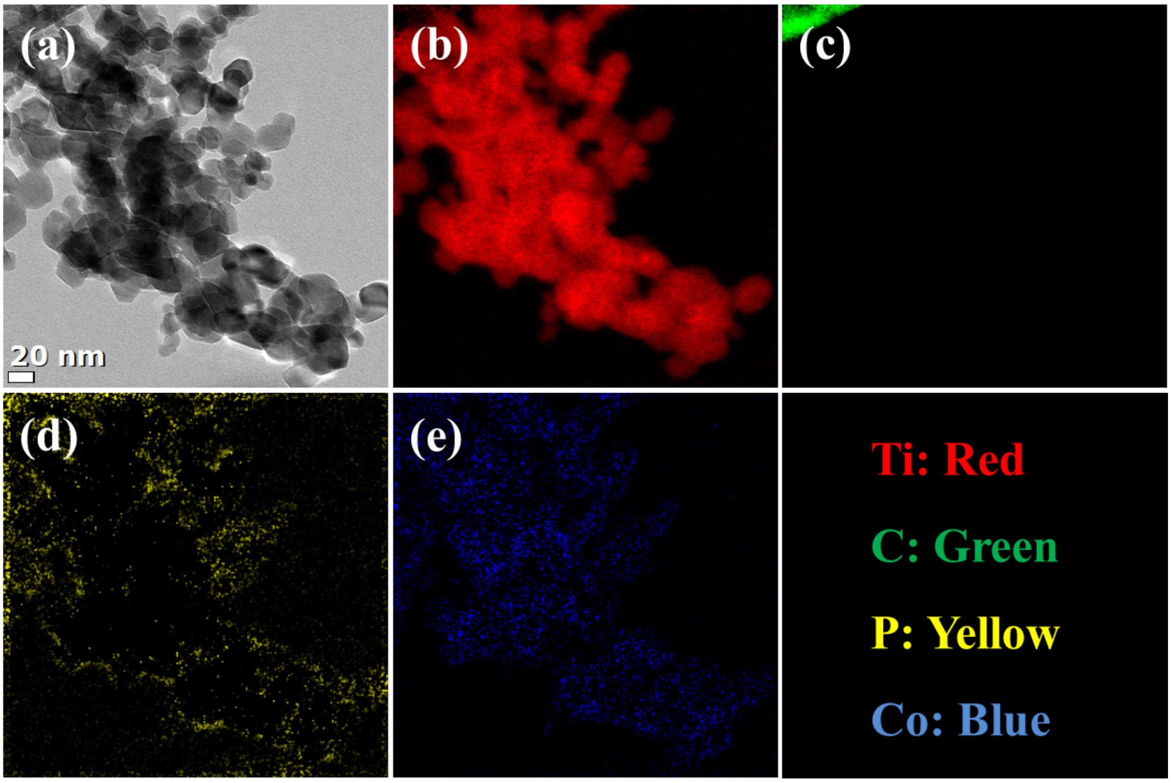

Fig. S10 (a) TEM image of TiO_2 after the irradiation for 3 hours in the presence of cobalt and phosphate ions. (b-e) EELS mapping corresponding to panel a. Red, green, yellow, and blue colors mean the existence of (c) titanium, (d) carbon, (e) phosphorus, and (f) cobalt elements, respectively.

References

1. H. Sheng, H. Ji, W. Ma, C. Chen and J. Zhao, *Angew. Chem.*, 2013, **125**, 9868.

2. *Catalytic Oxidations with Hydrogen Peroxide as Oxidant*, ed. G. Strukul, Kluwer Academic, Dordrecht, 1992.

3. R. Nakamura, A. Imanishi, K. Murakoshi and Y. Nakato, *J. Am. Chem. Soc.*, 2003, **125**, 7443.

4. P. Salvador and F. Decker, *J. Phys. Chem.*, 1984, **88**, 6116.

5. M. Suh, P. S. Bagus, S. Park, M. P. Rosynek and J. H. Lunsford, *J. Phys. Chem. B*, 2000, **104**, 2736.

6. Z. M. Qiang, J. H. Chang and C. P. Huang, *Water Res.*, 2002, **36**, 85.

7. I. Katsounaros, W. B. Schneider, J. C. Meier, U. Benedikt, P. U. Biedermann, A. A. Auer and K. J. J. Mayrhofer, *Phys. Chem. Chem. Phys.*, 2012, **14**, 7384.

8. G. Moon, Y. Park, W. Kim and W. Choi, *Carbon*, 2011, **49**, 3454.

9. H.-i. Kim, S. Kim, J.-K. Kang and W. Choi, *J. Catal.*, 2014, **309**, 49;

10. G. Moon, D. Kim, H. Kim, A. D. Bokare and W. Choi, *Environ. Sci. Technol. Lett.*, 2014, **1**, 185.